J Solid State Electrochem (2011) 15:1437–1450
DOI 10.1007/s10008-011-1369-9

REVIEW

Highlights of 20 years of electrochemical measurements of exocytosis at cells and artificial cells

Ann-Sofie Cans · Andrew G. Ewing

Received: 1 February 2011 / Accepted: 21 February 2011 / Published online: 4 May 2011

A.-S. Cans · A. G. Ewing (✉)
Department of Chemical and Biological Engineering,
Chalmers University of Technology,
41296 Gothenburg, Sweden
e-mail: andrew.ewing@chem.gu.se

Abstract Advances in electrochemical methodology over the past 30 years have allowed chemical measurements to be made with decreasing amounts of analyte and at smaller spatial dimensions. This has allowed the investigation of single cells and single vesicles in cells either during release of chemical transmitter or separately. The cellular event called exocytosis can be measured with amperometry or cyclic voltammetry as discovered by Wightman and first published in 1990. In addition, the measurement of vesicle contents with electrochemistry is a new approach we have termed electrochemical cytometry. This involves isolation of intact vesicles, separation of the vesicles, and then lysing followed by coulometric analysis of the electroactive vesicle content. In this review, we will highlight work done by us and by others to discuss measurements of exocytosis at single cells and measurements at artificial cell models for studying the biophysical properties of vesicle membrane dynamics and lipid nanotubes connecting artificial cells using electrochemical methods.

Keywords Vesicle · Exocytosis · Neurotransmitter · Carbon-fiber amperometry · Electrochemical cytometry · Artificial cell · Lipid nanotube

Introduction

Advances in methodology have allowed chemical measurements to be made with decreasing amounts of analyte and at smaller spatial dimensions. Indeed, this has often driven investigations at single cells providing unique chemical and biological insights at this fundamental level. In the central nervous system, cells communicate by the transmission of chemical signals between cells (neurotransmission). A neuron can form a specialized structure, called a synapse, through which neurons communicate with each other. This

communication is achieved when a cell releases signaling molecules. Following mass transport through the extracellular space between the cells, the molecules can bind to receptors, where they are recognized and a signal is transduced. The initial release event is called exocytosis and involves the fusion of a vesicle, filled with neurotransmitter molecules, with the cell plasma membrane. The signaling molecules in the vesicles are confined by a lipid bilayer; fusion with the plasma membrane creates a fusion pore, and the contents of the vesicle are released into the extracellular space. Mechanistic studies of this process are central to understanding neurotransmission. Therefore, methods have been developed to detect, measure, and characterize the release of molecules under both normal and experimental conditions.

One method used to measure molecules released during exocytosis involves the direct oxidation of these molecules, when they are electroactive, at the surface of an electrode. Typically, an electrode is placed on top of a cell and held at a constant potential that is sufficient to oxidize the analyte (typically <1.0 V vs. a Ag/AgCl reference electrode). The current generated by the oxidation is related to the number of molecules oxidized using Faraday's law. Thus, electrochemical methods are easily adapted to these measurements, and many investigations with this approach have been carried out yielding important information about exocytosis and neurobiology [1–14].

Bioanalytical techniques in general have been developed to measure chemical messengers from individual exocytosis events at single cells under in vitro experimental conditions [1, 5, 6, 12, 14–20]. Most of these methods can quantify kinetics of release and count events as well as in some cases indicate the location of release on the cell. Electrochemical methods are uniquely able to quantify the amount of chemical messenger released. In this article, we highlight the electrochemical methods that have been developed to measure exocytosis that have supported our understanding of this complex mechanism to date. Specifically, we focus on measurements at single cells and artificial cells.

Measurement protocols for exocytosis

Unraveling the dynamics of exocytosis is challenging because of the temporal and spatial domains in which these events occur. The volume of a synaptic vesicle is on the order of zeptoliters and can contain as few as several thousand molecules (zeptomoles of measurable material). Exocytosis is also a rapid process. A fusion event typically lasts from 0.1 to 100 ms, thus requiring high temporal fidelity in order to accurately measure the event. Finally, it is possible for cells to release multiple chemicals [21] making chemical identification of the compound a challenge as well.

The small scale of these measurements requires a method with a high signal-to-noise ratio. When designing an experiment, it can be helpful to take cues from nature to replicate the task. The postsynaptic cell in a synapse is able to "detect" the small number of signaling molecules released by the presynaptic cell because the restricted volume of the synapse minimizes dilution, the surface of the cell is sensitive to the neurotransmitter, and the signal depends on the concentration of neurotransmitter at the surface and not on the amount released. The electrode used for electrochemical measurement of these events must therefore be extremely close to the surface of the cell to match the distance of the synaptic cleft (sub-micron) to measure signals above the baseline noise. The capacitance of the electrode is a source of noise and is dependent on the electrode area, whereas the desired signal due to faradaic current is dependent on the amount of neurotransmitter released. This makes it important to restrict the area of the electrode surface to the confines of the surface of the cell being analyzed. Any superfluous surface area will contribute to the noise current without adding faradaic current. Thus, the small scale of these experiments requires small electrodes.

Measurements at single cells

Electrochemical measurements of neurosecretion have been the most quantitative dynamic assessment of the chemical messengers released during exocytosis to date. The utility of electrochemical methods to investigate neurobiological phenomena results from the fact that a select grouping of chemical messengers triggered during cell signaling processes are electroactive (e.g., dopamine, epinephrine, norepinephrine, serotonin, histamine, various neuropeptides, etc.) and therefore can be easily oxidized or reduced at a polarized surface (typically held at 0.2–1.0 V versus a Ag/AgCl reference electrode). The development of the voltammetric carbon-fiber microelectrode sensor [22] has made it possible to measure these messengers in biological microenvironments. This has served as a valuable tool for determining factors associated with the identity, amount, and time course of vesicular content secretion. The small double-layer capacitance of microelectrode sensors generates a rapid temporal response (microsecond) suitable for monitoring the dynamics of transmitter release in real time [23]. Furthermore, the size of these sensors (typically 5-μm tip diameter) permits spatial selectivity to screen for vesicular release in small regions of tissue or at single cells.

The first electrochemical measurements of individual vesicular release events at single cells were recorded by Wightman and coworkers on catecholamine-containing bovine adrenal chromaffin cells using constant potential amperometry at carbon-fiber microelectrodes [12]. This

work revolutionized the analytical investigation of exocytosis by providing a controlled method to quantitatively monitor the stimulus-coupled secretion of vesicular transmitter. Current transients observed from the electrooxidation of vesicular catecholamine released from a typical cell are shown in the amperometric trace in Fig. 1a. Nearly each current transient on an amperometric trace can be attributed to a discrete vesicle fusion event. The measured charge (Q) from current transients on the amperometric trace can be related to the mole amount of transmitter (N) detected per vesicle using Faraday's Law ($Q = nNF$), where n is the number of electrons exchanged in the oxidation reaction ($2e^-$ for most monoamines) and F is Faraday's constant (96,485 C/mol). These can be summarized for many events and plotted as a histogram of events at each amount released. Fig. 1b shows distributions for amperometrically measured amounts of transmitter detected from the induced exocytotic release of three commonly investigated large dense core vesicle-containing neurosecretory animal models (PC12 cells, human pancreatic beta cells, and rat mast cells) [14].

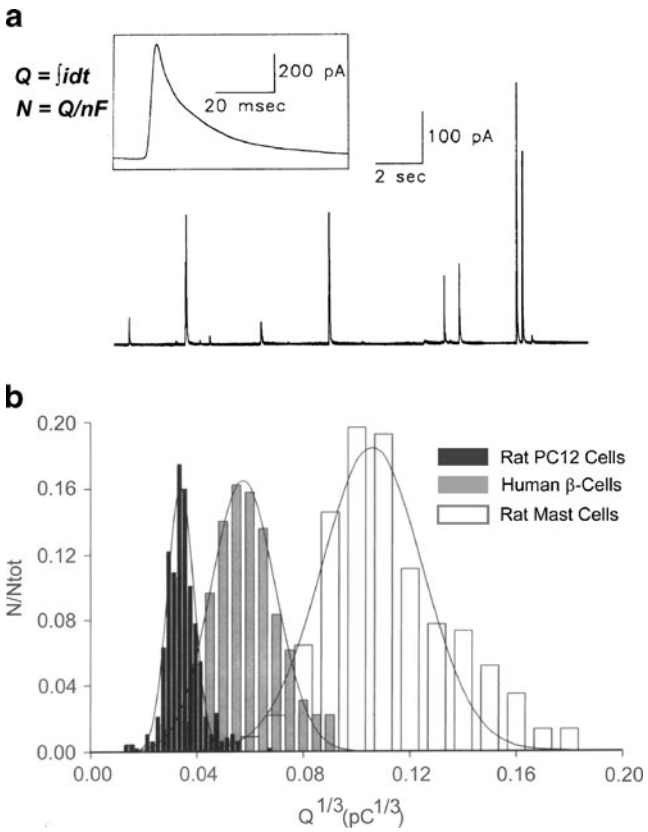

Fig. 1 Measurement of stimulus-coupled vesicular secretion using carbon-fiber amperometry at single cells. **a** Representative amperometric recording from the secretion of transmitter from LDCV-containing bovine adrenal chromaffin cells. Each spike identifies a single vesicle release event. *Inset* illustrates typical peak characteristics. Peak integration reveals the mole amount of transmitter released per vesicle. Adapted with permission from [13]. **b** Normalized frequency histogram revealing the amount of transmitter released from typical LDCV-containing animal models measured using amperometry at carbon-fiber microelectrode sensors. Q plotted as cubed root transform of amount to account for the spherical nature of the vesicle. Data are fit to Gaussian distributions to illustrate the heterogeneity of vesicular content from various secretory cells. Adapted with permission from [14]

There are two modes of electrochemical techniques used to measure release from single cells with carbon-fiber microelectrodes: amperometry and cyclic voltammetry. Amperometric measurements use a constant potential; the oxidation current is continuously monitored as the signaling molecules are released. In cyclic voltammetry, the potential is periodically scanned, and the current is recorded as a function of voltage. The curve produced, or cyclic voltammogram (CV), represents the characteristic oxidation and reduction potentials of the molecule at the electrode surface. This is a powerful method which can be used to identify a released molecule by comparing the CV to a standard CV. It can also be employed to discriminate molecules in a mixture [24]. In one report, chromaffin cells were stimulated, and successive cyclic voltammograms were collected at a carbon-fiber microelectrode (Fig. 2). Data were collected at a rate of 50 cyclic voltammograms per second, allowing resolution of individual release events. The cyclic voltammograms can be plotted as "color plots," where the x-axis is time, the y-axis is applied potential, and the current is represented in false color. In this case, principal component regression was used to chemically identify the released molecules as either epinephrine or norepinephrine.

Both amperometry and cyclic voltammetry can be used to collect data at a rate sufficient to temporally resolve individual exocytosis events. However, amperometry has exceptional temporal resolution affording the ability to obtain precise information about the kinetics of the release event. The rise time of the peak is related to the time required for the vesicle to open after initial fusion, the peak width at half the maximum is used to measure the duration of the event, the amplitude gives the maximum flux of signaling molecules released, and the decay time is related to the diffusion of the molecules. These metrics have been used to compare the effects of exogenous agents such as drug treatments [25–27], neurotoxins, and non-native lipids [3, 10].

The electrochemical measurement carried out by placing a carbon-fiber microelectrode on the cell surface to quantify exocytosis was first demonstrated by Wightman et al. [8, 12]. In this early experiment, bovine chromaffin cells were induced to undergo exocytosis by exposure to nicotine, carbamylcholine, or potassium ion delivered with a pressure pulse from a micropipette. The released chemicals were quantified with amperometry and identified as catecholamines with cyclic voltammetry. Catecholamines are an important class of neurotransmitter that includes

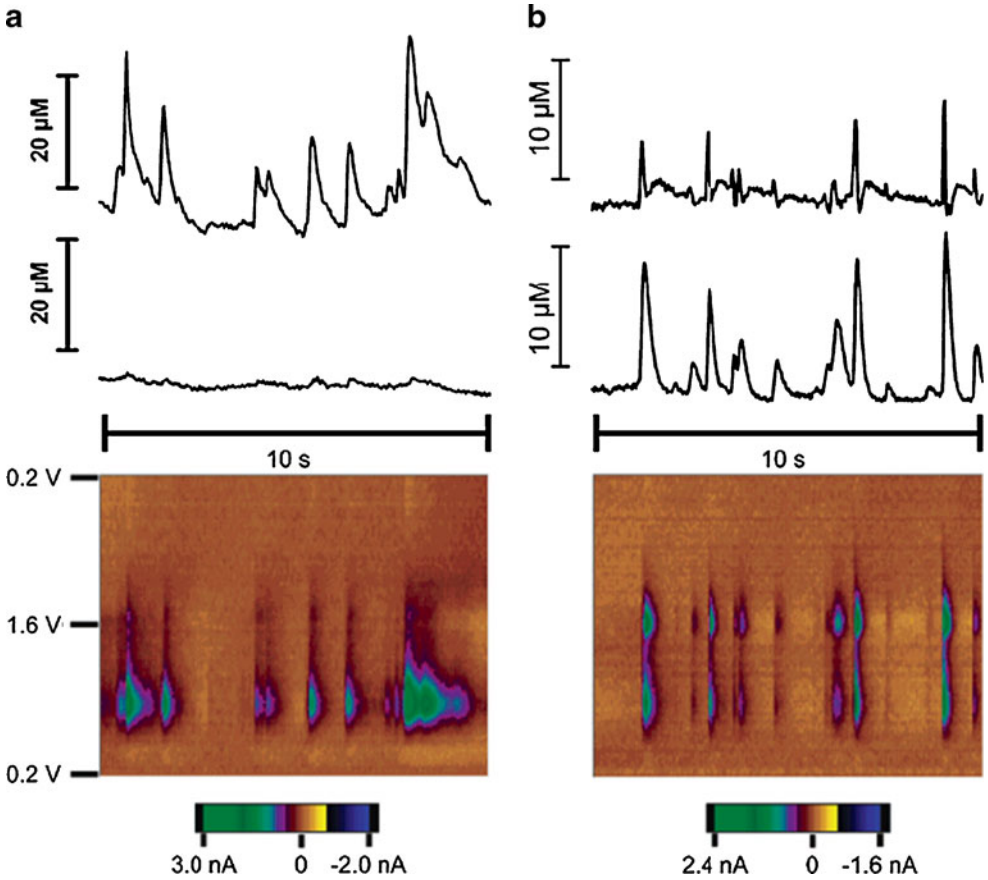

Fig. 2 Vesicular release events measured at individual cells. **a** *Lower panel* color representation of release from a single cell. The *upper trace* is the concentration of norepinephrine assigned by principal component regression, and the *middle trace* is the epinephrine assignment. **b** *Lower panel* release measured at another cell. The *upper trace* is the norepinephrine prediction, and the *middle trace* is the epinephrine assignment. Reproduced with permission [24]

dopamine and adrenaline (epinephrine). An increase in the frequency of the spikes was clearly observed following stimulation of vesicle fusion. Fusion events depend on the availability of Ca^{2+} [28], and if the Ca^{2+} is removed from the buffer, no spikes are observed. Amperometric spikes measured in the presence of Ca^{2+} have distributions of areas around a mean. This matches well with the description of exocytosis as discreet chemical release events from a population of similar-sized vesicles. More evidence for quantized release is that the intensity of the stimulation has no effect on the area of the spikes; it does, however, have a direct relationship to the frequency of the events. Finally, the area of the peak can be used to calculate the amount of material detected, and the values obtained agree with the average number of catecholamine molecules expected to be inside of a single chromaffin cell vesicle.

Cyclic voltammetry can also be used to identify two catecholamines co-released from individual adrenal medullary chromaffin cells. These cells are known to release both epinephrine and norepinephrine [29], thus, cyclic voltammetry has been used to determine the chemical composition of individual events [21]. These data show that the cells fall into three subcategories—cells that primarily release epinephrine, cells that primarily release norepinephrine, and a small group of cells that release a combination of the two. This work showcases the chemical specificity of cyclic voltammerty and the importance of single cell investigations as subgroups would have been unobservable if the total population was investigated simultaneously.

Measurements of the dynamics of the fusion pore opening during exocytosis

Amperometric transients from exocytosis are often preceded by a small pedestal, called the "foot" of the spike [1, 6]. Combined patch-clamp and amperometric measurements have confirmed that the foot represents neurotransmitter release through the fusion pore in beige mouse mast cells [1]. Furthermore, in chromaffin cells, the catecholamine released during the amperometric foot and during the main portion of the spike is the same [13], thus confirming the existence of a dynamic fusion pore.

The fusion pore is the molecular structure that connects two cellular membrane compartments during their fusion. All vesicle trafficking occurs through the formation and dispersion of fusion pores. Intracellular compartments transport materials through fusion pores, and by controlling the exchange of phospholipids and proteins through the lips of fusion pores, cells have the capability to selectively maintain the composition of an intracellular compartment. Exocytotic release occurs through a fusion pore, the

exocytotic fusion pore, which forms a continuous aqueous connection between the vesicle lumen and the extracellular space for the extrusion of vesicle contents. As the fusion pore forms, the vesicle membrane merges with the plasma membrane. Since the fusion is created between the extracellular and intracellular compartments, it is well suited to study with electrophysiological, electrochemical, and fluorescent methods. Owing to the use of these methods, our understanding of fusion pore dynamics has developed dramatically during the past few decades.

The earliest efforts to profile fusion pores employed electron microscopy of quick-freezing frog neuromuscular junctions [30–32]. These pictures indicated narrow fluid connections between the vesicle and the cell exterior with diameters as small as 20 nm [32]. In addition to the data from nerve terminals, Chandler and Heuser [33] captured fusion pores in degranulating mast cells by quick-freezing techniques. Their data showed membrane-lined pores of 20 to 100 nm in diameter that provided aqueous channels connecting the granule (vesicle) interior with the extracelluar space. More recently, the advent of atomic force microscopy has provided new insights into the structure of fusion pores [34]. The early work of Heuser and Reese stressed the existence of fusion pores. Electrical recording from living cells in the act of secretion ultimately allowed some small determination of the nature and properties of the initial fusion pore.

Studying the fusion pore in living cells with electrochemistry

The dynamics of the fusion pore have been mainly investigated at the level of single cells by two techniques: the patch-clamp method, measurements of the electrical capacitance of cell membrane [35–37], and the amperometric method for quantifying catecholamine neurotransmitter release with carbon fibers discussed here [1, 6, 12, 16]. Whereas patch clamp detects changes of cell membrane area and conductance due to vesicular fusion, the electrochemical method measures the currents produced during oxidation of released secretory products from each exocytotic event and can be used to quantify the number of moles released.

Contemporary measurements with amperometry and transmission electron microscopy to understand the existence and dynamics of the fusion pore are shown in Fig. 3. As stated above, release through a stable fusion pore is distinguished in amperometric signals of exocytosis as a prespike foot. The integrated area under the foot portion of the spike is representative of the number of molecules released through the fusion pore, prior to full fusion. The duration of release during the foot is indicative of the lifetime, or stability, of the fusion pore structure.

Finally, the frequency with which amperometric feet are observed is a direct measure of the frequency with which vesicles release neurotransmitter through a stable exocytotic fusion pore as an intermediate state, as opposed to explosive vesicular fusion. Data from PC12 cells indicate that vesicular volume before secretion is strongly correlated with the characteristics of amperometric foot events [38]. Treatment with reserpine and L-3,4-dihydroxyphenylalanine have been used to decrease and increase, respectively, the volume of single pheochromocytoma cell vesicles [7]. Exposure of PC12 cells to 100 μM L-DOPA for 90 min significantly decreases the observed frequency of foot events to 72% of control [38]. In contrast, when PC12 cells are treated for 90 min with 100 nM reserpine, there is an increase in the frequency of foot events to 155% of the measurements at control cells. Under control conditions, an average of ~33.7±0.5% of the exocytotic events from PC12 cells exhibits a prespike feature. Thus, a clear trend exists in relating the frequency of foot events to vesicular volume. Further analysis indicates that (1) both foot duration and foot area are directly related to the physical size of the vesicle (Fig. 4) and (2) the percentage of the total contents released in the foot portion of the event is dependent on vesicle size.

Interestingly, smaller vesicles display a foot in the amperometric record more frequently than the control. We hypothesize that this result is largely an effect of the membrane tension differential that exists across the fusion pore. Immediately following vesicular fusion with the plasma membrane and pore formation, the vesicular dense core swells apparently, resulting in release of core-bound transmitter but also applying pressure to the vesicular membrane. Because the dense core of a reserpine-treated vesicle largely fills the vesicle, core expansion should increase the vesicular tension to a greater extent than in the control case, where the core does not occupy as much of the overall vesicular volume. The resultant tension differential across the pore induces transient pore stabilization until membrane flow relieves this tension and further distention of the vesicle can occur. Thus, the fusion pores of smaller vesicles would appear to be more significantly stabilized, and amperometric feet occur in the data record more frequently.

Studying fusion pore in artificial cells with amperometry

Besides living cells, artificial cell models have contributed a great deal to our understanding about membrane fusion [39–41]. A common model has involved vesicles containing channel proteins that are driven by osmotic pressure to fuse with a planar lipid bilayer [42, 43]. An adaptation of

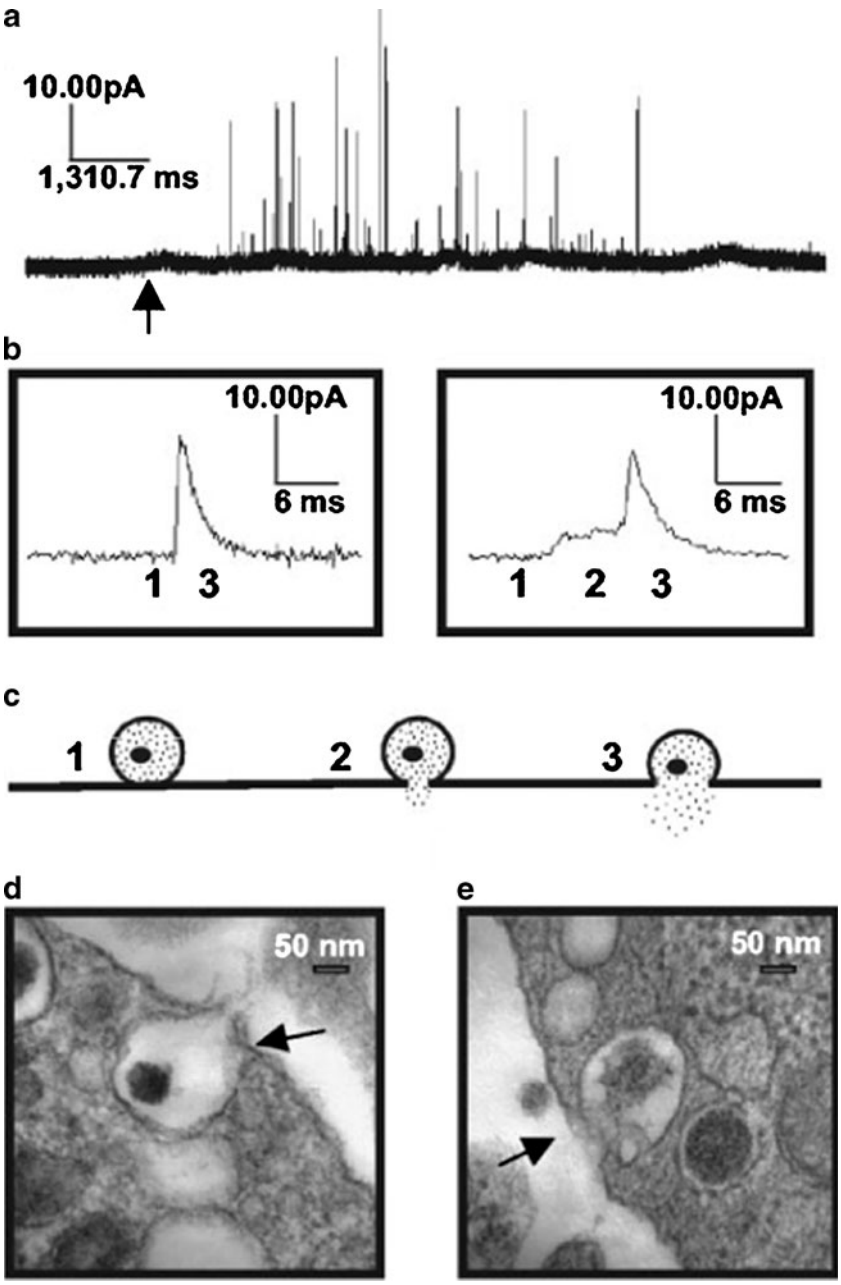

Fig. 3 **a** Representative amperometric data from a single PC12 cell. The *arrow* under the trace represents the time of stimulus (100 mM K^+) application. **b** Examples of individual amperometric current transients. The *trace on the left* has no discernable foot signal; that on the *right* is preceded by a foot. **c** A schematic diagram illustrating the flux of neurotransmitter through the fusion pore. The stages of fusion are numerically coordinated with the associated regions of the amperometric traces in **b**. **d** and **e** Representative TEM images of PC12 cell dense core vesicles fusing with the plasma membrane on stimulation with 100 mM K^+. *Dark arrows* indicate vesicles that appear to be undergoing exocytosis. *Scale bars* are 50 nm. Reproduced with permission [38]

this model has been used to demonstrate transient opening of fusion pores in protein-free membranes, suggesting that indeed proteins might not be needed for this process [44]. Recently, we used electroinjection technology to develop a protein-free liposome system as an artificial cell that undergoes exocytosis [45–47]. Fluorescence microscopy and amperometry were used to detect leakage of transmitter through a nanoscopic fusion pore and quantal release during the final stage of exocytosis.

Figure 5 shows a vesicle formed inside a surface-immobilized liposome via electroinjection. A micropipette filled with a solution of electroactive substance is inserted into the center of a giant unilamellar vesicle by electroporation and from inside and out is electroporated to allow the tip to penetrate to the outside (Fig. 5a, b). When the lipid membrane has sealed around the pipette tip, the pipette is retracted into the liposome pulling in a lipid nanotube that is attached between the tip of the pipette and the membrane of the giant liposome (Fig. 5c). By continuously injecting solution into the lipid nanotube, a vesicle is inflated like a balloon at the tip of the pipette (Fig. 5d). As the vesicle grows, the lipid nanotube decreases in length until the length of the lipid nanotube is so short that a toroidal shape, similar to the structure of a fusion pore, remains. This is not a very stable structure and forces the inner vesicle to dilate and to release the solution

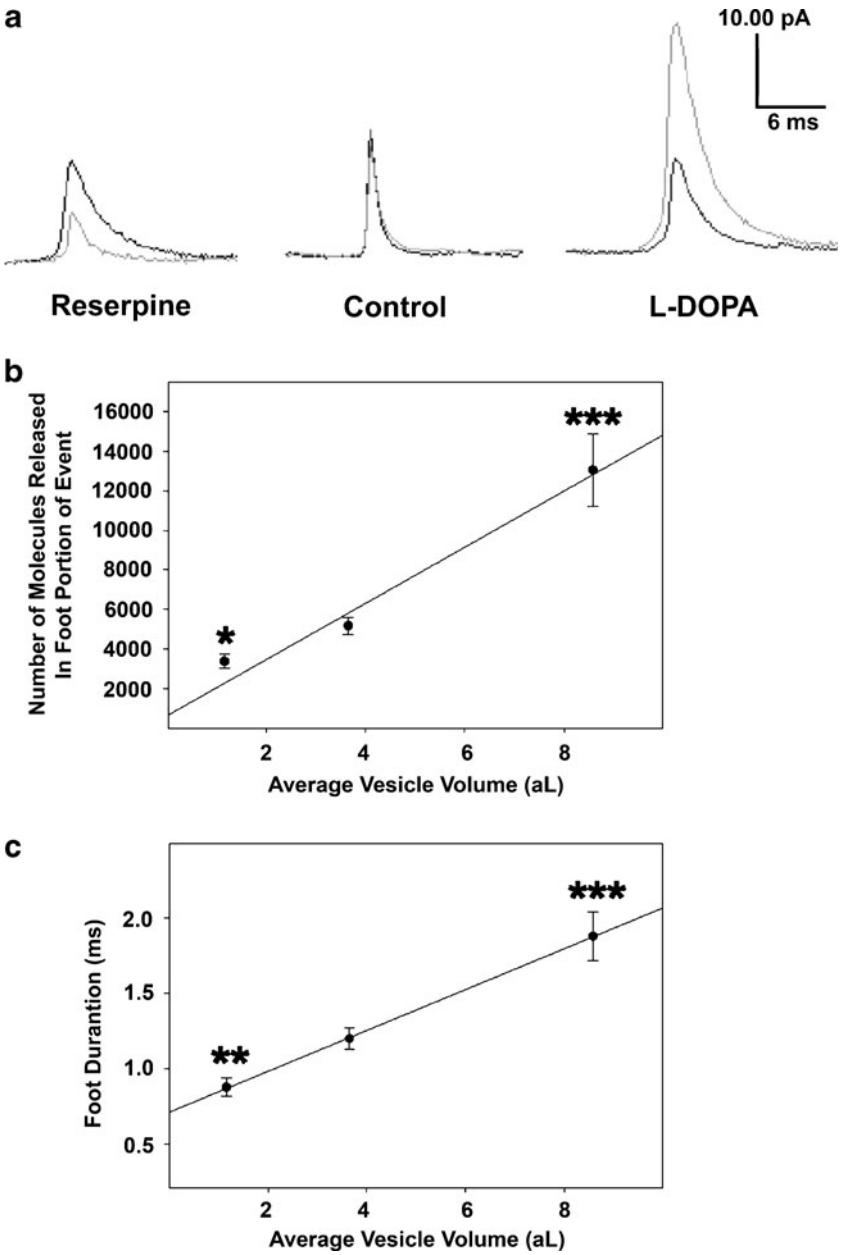

Fig. 4 Both the number of molecules released through the exocytotic fusion pore and the time course of said release are dependent on vesicular size. **a** Averaged amperometric current transients for one reserpine-treated, saline-treated, or L-DOPA-treated PC12 cell before (*black*) and after (*gray*) the 90-min incubation period. The *scale bar* is the same for all three averaged transients. **b** Mean foot area values shown as a function of vesicle volume. Under control conditions, a cellular average of 5695±751 molecules was released through the fusion pore (before full fusion) per event. **c** Mean foot duration values (the time lapse between the onset of the foot and the inflection point between the foot and the full fusion event) shown as a function of vesicle volume. Under control conditions, the average cellular time course for release through the fusion pore was 1.3±0.1 ms. *Error bars* represent the mean ± SEM of the foot characteristic values for the different experimental conditions. *$p<0.05$, **$p<0.01$, and ***$p<0.001$ versus control, respectively (*t* test). Reproduced with permission [38]

containing electroactive substance at the surface of the electrode. This is shown schematically in Fig. 5f–i and by monitoring of fluorescence in Fig. 5j–m. Amperometric traces for this process are shown in Fig. 6a. The different stages are indicated on an example amperometric trace in Fig. 6b, and this will be discussed below in terms of the fusion pore. In comparison to vesicles fusing during exocytosis in living cells, the sizes of the inner vesicles here are approximately ten times larger and can therefore be visualized by video microscopy. Visual evidence showed that release occurs in a similar manner to that suggested for vesicle release at cells during exocytosis. The time course of vesicle release for the smallest artificial vesicles was found to be in the same range as the time course for exocytosis from mast cells, where the vesicles are comparable in size to the model. Conclusions were that proteins are not needed for the later stages of exocytosis as the membrane dynamics alone are sufficient to drive the vesicle dilation. This artificial cell model was further used to study the properties of a fusion pore.

The nanotube initially resembles an elongated fusion pore and was used to model molecular leakage through

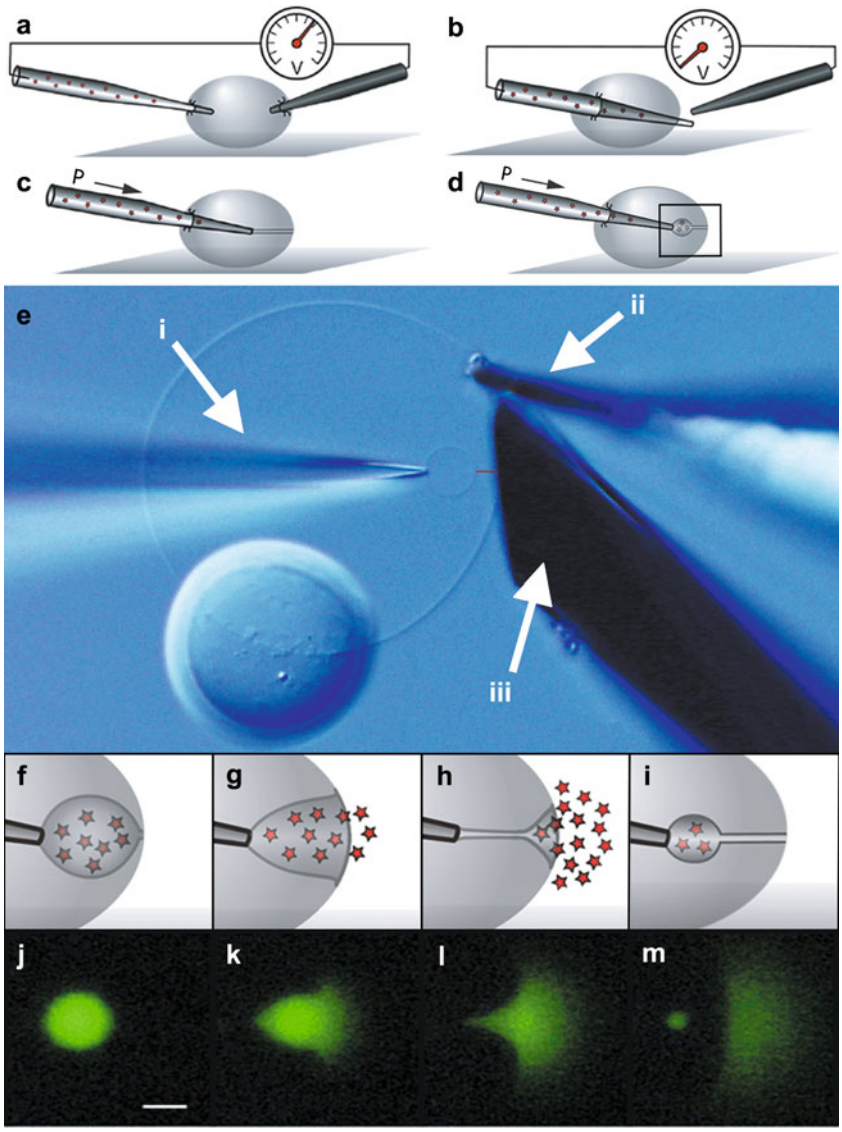

Fig. 5 Formation and release of vesicles in an artificial cell. **a**–**d** Schematics of a microinjection pipette electroinserted into the interior of a unilamellar liposome and then through the opposing wall, pulled back into the interior, followed by spontaneous formation of a lipid nanotube and formation of a vesicle from flow out of the tip of the micropipette. **e** Nomarski image of a unilamellar liposome, with a multilamellar liposome attached as a reservoir of lipid, microinjection pipette (*i*), electrode for electroinsertion (*ii*), and 30-μm diameter amperometric electrode beveled to a 45° angle (*iii*). A *small red line* depicts the location of the lipid nanotube, which is difficult to observe in the computer image with a ×20 objective, illustrating a vesicle with connecting nanotube inside a liposome. **f**–**i** Fluid injection at a constant flow rate results in growth of the newly formed vesicle with a simultaneous shortening of the nanotube until the final stage of exocytosis takes place spontaneously and a new vesicle is formed with the attached nanotube. **j**–**m** Fluorescence microscopy images of fluorescein-filled vesicles showing formation and final stage of exocytosis matching the events in **f**–**i**. *Scale bar* represents 10 μm. Reproduced with permission [45]

the pore before vesicle dilation. In Fig. 6a, several amperometric traces are shown for measurement at the artificial cell with an obvious prespike signal shown. The different parts of the release are shown in Fig. 6b as indicated above, and this includes the concept of release via the fusion pore. This was done by studying the effects of different pressures during microinjection into the pulled lipid nanotube. Microinjection of solution into the tube leads to a local increase in membrane tension and thus to a reduction in this tension difference. Lipid material then flows from regions of lower tension (outer membrane) along the nanotube toward higher tension, forming the membrane of the small vesicle. Data from the artificial cell system suggest that the time course for leakage (foot length) through the fusion pore is governed by injection flow rate, as determined by pipette pressure, and is proportional to the size of a vesicle immediately before release (Fig. 6c). The total amount of material leaking through the lipid nanotube (foot area) is proportional to vesicle size at the stage directly before release but is independent of injection flow rate (Fig. 6d), indicating that nanotube length is the critical parameter determining total leakage. However, at any given vesicle size, the rate of leakage through the lipid nanotube (foot area/foot length) varies with flow rate (pipette pressure) and vesicle size (Fig. 6e). These observations can be explained by considering the sources of liquid flow inside the nanotube (Fig. 6f). Lipid is transported from the artificial cell into the vesicle during expansion, resulting in shear flow of the liquid column inside the nanotube and toward the vesicle. In contrast, solution pressure from the pipette results in Poiseuille flow from the interior of the vesicle that opposes the direction of the shear flow. These results support the conclusion that the rate of fluid transport

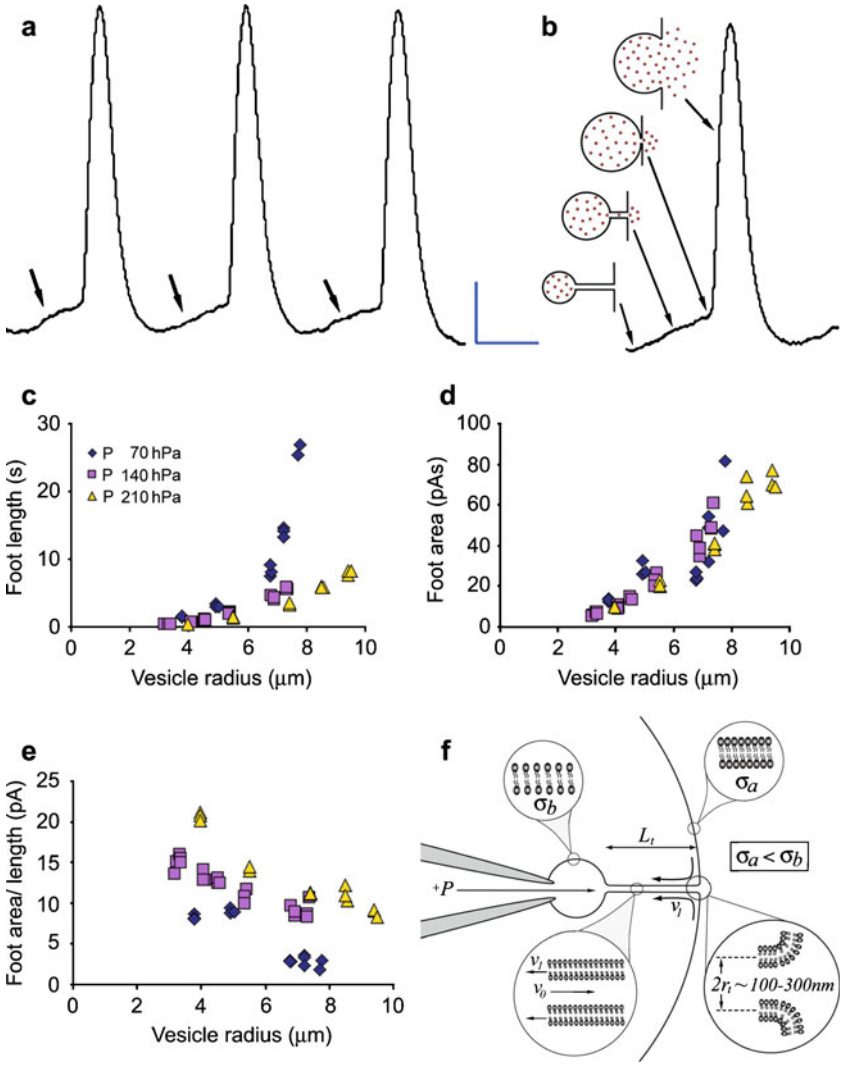

Fig. 6 Amperometric monitoring of release via an artificial fusion pore. **a** Amperometric detection of release from a 5-μm-radius vesicle showing prespike feet (*arrows*), indicating catechol transport through the lipid nanotube or fusion pore. *Scale bar* is 80 pA×500 ms. **b** Time correlation of vesicle growth, transport of transmitter through the lipid nanotube, and the final stage of exocytosis with amperometric detection. **c**–**e** Plots of foot length (**c**), foot area (**d**), and the ratio of foot area over foot length (**e**) observed with amperometry for vesicles fusing with an artificial cell at three different pressures used to inflate the vesicles. **f** Schematic model of the factors affecting flow in the vesicle and nanotube of the artificial cell. Reproduced with permission [45]

through the nanotube in the model cell depends on the length of the lipid nanotube and the factors affecting the counterbalance of shear and Poiseuille flow in the nanotube.

The data from the artificial cells are strikingly similar to what is observed during exocytosis in cells. Thus, the bottom-up approach in designing an artificial cell model can be used to examine fundamental aspects of exocytosis with a great deal of control of many experimental degrees of freedom. These include membrane and solution composition, differential pH values across vesicle membranes, temperature, and vesicle size.

Applications of electrochemical measurements of exocytosis

The electrochemical method has been applied to a number of secretory cell models for the investigation of vesicular release in real time to measure differences in the transmitter content of vesicles from brain [17–19] and peripheral cells [1, 14–16], as well as in a nerve cell of a living organism [5]. Carbon-fiber amperometry at microelectrode sensors has also been widely used to probe variations in vesicular transmitter loading and release resulting from manipulations of protein expression [48–50] and pharmacology [51–54].

Carbon-fiber amperometry has also been used to unravel various intracellular biophysical processes that contribute to the mechanism of release. The extraordinary temporal characteristics of amperometric recordings at single cells have successfully resolved momentary features of exocytosis such as those related to the formation of the fusion pore observed as a prespike foot as discussed above [1, 6, 55]. Amperometry at single cells has also been used to identify partial vesicular release events that involve "flickering" fusion pores [19] and kiss-and-run exocytosis. This concept is shown in Fig. 7a and

examples in Fig. 7b–c [1, 6]. Figure 7b shows the amperometric signature for a flickering fusion pore, where each of the spikes on the complex transient is assigned to a unique flickering event in which the fusion pore connecting the vesicle inside to the exterior is intermittently opened and closed [19]. Mechanisms of partial release have been supported in the literature through hybrid experimental techniques that couple amperometry with capacitance measurements (e.g., patch amperometry [1, 15, 56]) to measure changes in membrane area in tandem with secretion. Partial release models of exocytosis support the interesting contention that transmitter secretion can be regulated from single vesicles, which imparts a potential molecular basis for synaptic plasticity at the subcellular level and provides an explanation for the rapid membrane recycling necessary to efficiently drive the synaptic vesicle cycle to completion [57].

An emerging trend in neurosecretory analyses has revolved around developing technologies capable of electrochemically resolving the location of active release sites on secretory cells. Electrochemical methods to quantitatively map "hot spots" of vesicular release have included the use of dual microelectrode sensors [58], microelectrode arrays (MEAs) [59], and electrodes spatially located below and above the cell [60] to study exocytosis. In a recent report by Zhang et al., a multi-barrel array of seven individually addressable carbon-fiber microelectrodes was fabricated and used to map the spatiotemporal vesicular release characteristics at stimulated PC12 cells (Fig. 8a) [59]. The individual electrodes (2.5-μm radius) were constructed in a multi-barrel glass capillary, pulled to a fine tip to form an array, and polished to an angle for adequate placement on the target cell. This resulted in a MEA possessing a total diameter of about 20 μm, a dimension suitable to encompass the entire surface of a typical cell for somatic release recordings. The current traces in Fig. 8a represent amperometric recordings from each of the individually addressed electrodes in the MEA array elicited via chemical stimulation of a PC12 cell. This approach allows the heterogeneity of release observed from various regions of the cell to be resolved by providing a quantitative assessment of measured transmitter. Amatore and coworkers electrochemically investigated the frequency, kinetics, and content of vesicular release from both the apex and base of bovine adrenal chromaffin cells [60]. This was accomplished by coupling conventional amperometry with a carbon-fiber microelectrode and measurements at a thin film indium tin oxide electrode (ITO) placed below the cell. The experimental platform is depicted in Fig. 8b, where adrenal chromaffin cells are cultured on the ITO electrode surface and subsequently subjected to stimulus-coupled secretion. An overall higher amount of vesicular content released was observed from the basal pole when compared to the apical pole of the cell, possibly suggesting that sampling was achieved from distinct vesicle pools, although the different electrode materials might play a role as well.

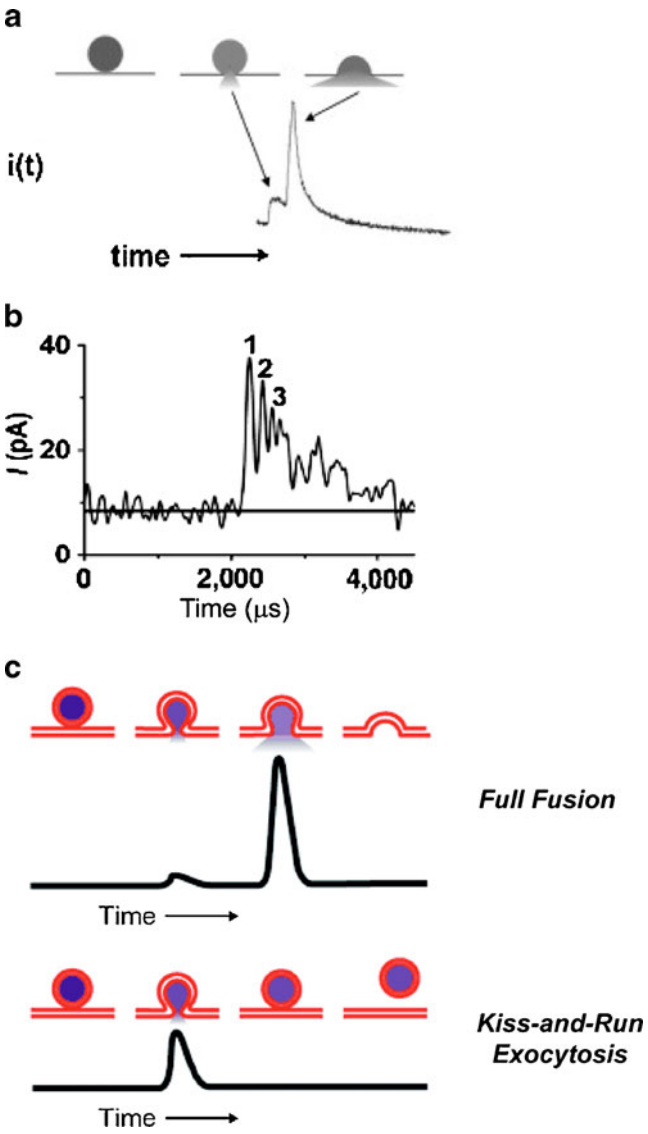

Fig. 7 Biophysical mechanisms of vesicular release can be elucidated from amperometric measurements at carbon-fiber microelectrodes. **a** Proposed mechanism and representative trace that depicts a prespike "foot". It is proposed that the small rise in current that precedes the distention of vesicular contents is due to formation of the fusion pore. This is followed by a large spike, which has been associated with full collapse of the vesicle membrane and expulsion of the transmitter contents. Adapted with permission from [69]. **b** Amperometric trace that displays a "flickering" fusion pore recorded from the stimulus-coupled secretion of dopaminergic mouse neurons. It is proposed that upon fusion with the plasma membrane, the fusion pore intermittently opens and closes as indicated by the complex peak observed. Each label on the complex event is assigned to a unique flickering event. Adapted with permission from [19]. **c** Cartoon depicting the mechanism of kiss-and-run exocytosis. This mechanism indicates partial release of a vesicle's content and can be resolved using electrochemical measurements as depicted in the simulated traces. Adapted with permission from [70]

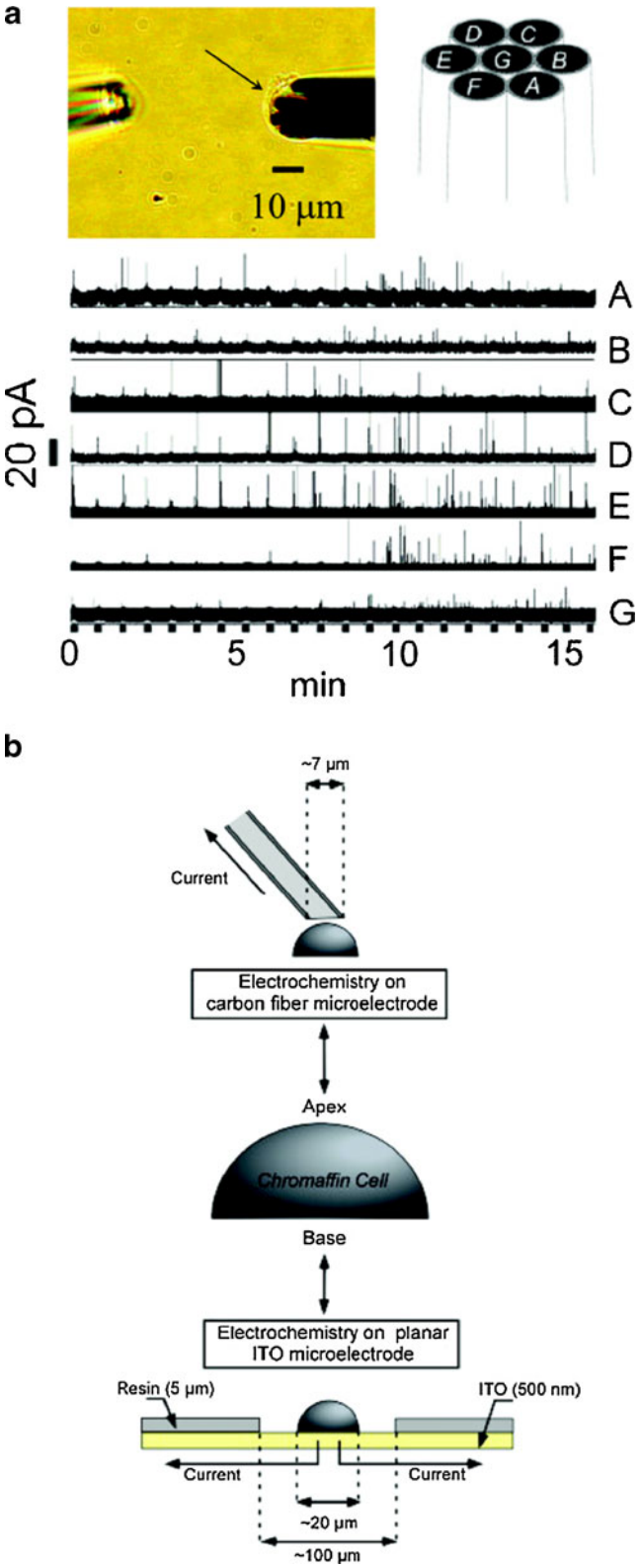

Fig. 8 New technologies developed to electrochemically map the location of active release sites on single cells. **a** MEA composed of seven individually addressable carbon-fiber microelectrodes. Bright field image of the sensor on a PC12 cell is indicated by the *arrow*. To the *left* of this image is a micropipette containing elevated K^+ solution to stimulate release. Shown *below* are representative amperometric traces recorded from each of the electrodes, demonstrating the heterogeneity of vesicular release across the cell surface. Adapted with permission from [59]. **b** Electrochemical measurements of stimulated vesicular release from both the apex and base of chromaffin cells. Conventional carbon-fiber amperometry techniques are combined with amperometry measurements at a thin film ITO electrode upon which cells are cultured. Adapted with permission from [60]

Electrochemical cytometry

We have developed a new technology termed electrochemical cytometry to quantitatively probe the transmitter content of individual secretory vesicles isolated from the cell environment via end-column electrochemical detection (CE-EC). Although conventional CE-EC has been used to quantitatively detect chemical messengers present in cytoplasm of single cells [61], it has been difficult to differentiate between the presence of cytosolic and vesicular transmitter in the resultant electropherograms. The novel electrochemical cytometry device provides the means to directly interrogate vesicular content using a hybrid capillary-microfluidic platform (Fig. 9) [62, 63]. In this process, secretory vesicles are first isolated offline from tissue homogenates using differential centrifugation. They are then electrokinetically injected onto a fused-silica capillary and subsequently isolated as individual entities by electrophoresis. The separation capillary terminates into a PDMS-based microfluidic device that continuously delivers lysis buffer to the detection zone in sheath-flow format. As individual intact vesicles exit the separation capillary, they are lysed and amperometrically detected at a cylindrical carbon-fiber microelectrode positioned at the outlet.

The electrochemical cytometry device has been characterized using artificial vesicles both containing and lacking an electroactive analyte in order to highlight both the sensitivity and selectivity of the detection scheme (coulometric efficiency >95%) [60]. In a more recent study, quantification of LDCV content has been accomplished for PC12 cell vesicles [63]. A 1,000-s portion of a representative electropherogram from these data is shown in Fig. 9b, as well as an expanded view of the axis in order to illustrate the typical peak characteristics. The resultant peaks can be integrated and subsequently related to the amount of transmitter per vesicle as described earlier in this article for amperometry at single cells. The electrochemical cytometry device provides a high-throughput approach for the measurement of vesicular content from the entire cell (>5,000 vesicles detected in a typical run with about 1 nL of suspension injected versus ~100 vesicle release events with conventional single cell amperometry experiments for a single stimulation per cell). Moreover, the electrochemical cytometry measurements have provided information about the total content of vesicular transmitter, which has been compared to data from release experiments at single cells to

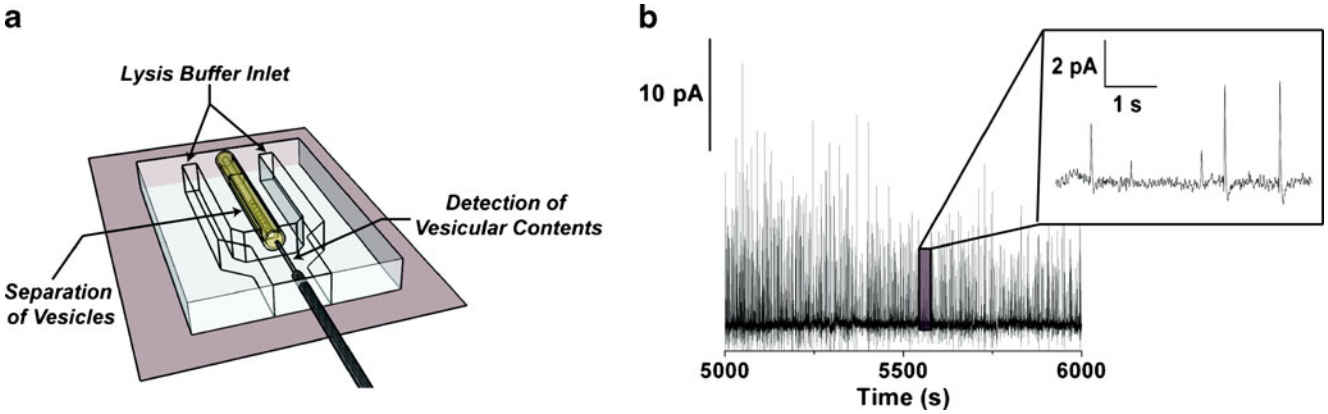

Fig. 9 Electrochemical cytometry to quantitatively probe individual secretory vesicle transmitter content in a high-throughput manner. A schematic illustration of the device is presented (not drawn to scale) in (**a**). A 1,000-s portion of a representative electropherogram that demonstrates the separation, lysis, and electrochemical detection of transmitter content from individual vesicles is shown in (**b**). *Inset* contains an expanded axis to depict typical peak characteristics

determine that only 40% of a vesicle's content is expelled during the average exocytosis event, a premise that quantitatively contradicts classical hypotheses of all-or-none quantal release [63].

Electrochemical measurements of the inside diameter of lipid nanotubes

In addition to the fusion pore discussed above, lipid nanotubes are found in cells and might be involved in intracellular transport or in connections between cells during genetic exchange [64–67]. To learn more about the biophysical properties of highly curved lipid in lipid nanotubes, we developed an electrochemical method to measure the diameter of these nanotubes [68]. This method involves insertion of a micropipette filled with electroactive solution to the inside of a giant unilamellar and pulling a lipid nanotube connecting the tip of the micropipette and the vesicle membrane. This is performed in the same manner as described in Fig. 5a–c; however, zero pressure is applied to the micropipette. By placing a carbon-fiber microelectrode close to the membrane of the giant vesicle, positioned at the opening of the nanotube, the steady-state amperometric current can be measured by oxidizing the molecules diffusing from the micropipette, through the lipid nanotube. Assuming the concentration gradient is linear through the tube, the change in baseline current (Δi) is measured for diffusion of molecules through the tube at different nanotube lengths and is compared to the steady-state current measured in the bulk solution, away from the vesicle, and a simple equation using Fick's law can be used to calculate the cross-sectional area of the tube. A trace from one nanotube experiment is shown in Fig. 10. The model allows for measurements of lipid nanotube dimensions at different lengths by determining the distance the micropipette is pulled from the membrane before measurement. Our data show that at longer tube lengths (>10 μm), the tube dimension is fairly constant; however, at shorter lengths, the nanotube is constricted. We also compared the nanotube connected between a micropipette tip and the giant vesicle membrane to a tube connected between a smaller vesicle inflated at the tip of the micropipette and the giant vesicle. These measurements showed that when a lipid nanotube is connected between two vesicles, the tube

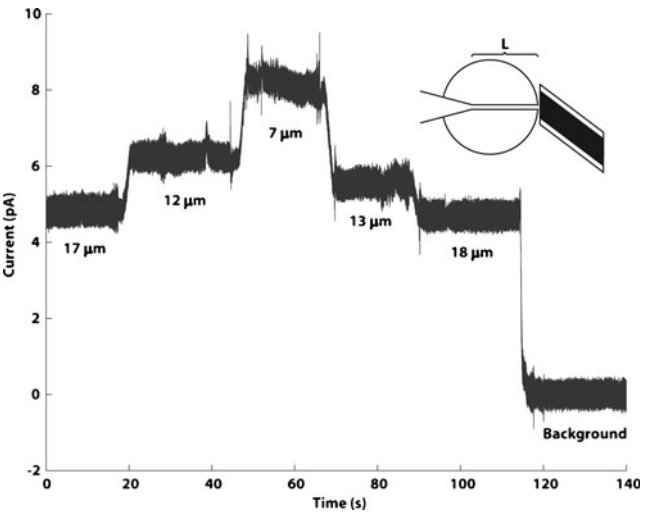

Fig. 10 Steady-state amperometry is used to detected electroactive molecules diffusing from the micropipette through the lipid nanotube and to the outside by oxidizing them at the surface of the carbon-fiber microelectrode held at a potential of 0.7 V vs. an Ag/AgCl reference electrode. By varying the micropipette distance from the vesicle membrane, the steady-state current is measured at different lipid nanotube lengths and is compared to the steady-state current measured in the background of the bulk solution at far distance from the vesicle. From this trace, the Δi can be calculated. Adapted with permission from [68]

constricted to a higher degree than when attached to a micropipette. This suggests that the attachment to two high curvature neck regions of the two vesicles promotes restriction of the lipid nanotube cross section. This bottom-up approach method allows for measurements of the dimensions of a lipid nanotube where membranes can be studied as a function of, e.g., lipid composition, the effect of including specific proteins in the membrane, and lipid phase domains.

Conclusions

Electrochemical measurements at single cells have provided the most chemically quantitative dynamic assessments of the spatiotemporal aspects of exocytosis to date. Further, emerging technologies in electroanalytical chemistry have opened up the possibility of quantitatively imaging exocytosis via the development of novel sensors capable of electrochemically mapping active vesicular release sites on a cell surface. A new method, electrochemical cytometry, has been used to measure total transmitter content for vesicles isolated from the cell environment, and when compared to conventional stimulus-coupled secretion events at single cells, the fraction of transmitter released during exocytosis has been determined to be less than unity. A great deal of the work in this area has been focused on measuring events through the fusion pore created as a vesicle begins to fuse with the cell membrane. In this regard, it is interesting to model this with artificial cell methods, and we have done this and shown how a simple Fick's law approach can be used to determine the size of nanotubes.

The work described here is only a small part of that taking place, and we focused on our own interests here. A great deal of exciting work is currently ongoing from both the developmental aspect and the application of this relatively new technology to cell and neuroscience. In the future, again from our perspective, we envision individually addressed arrays with much higher density for real cell imaging. We envision analysis of large numbers of much smaller vesicles taken from cells. In addition, there is a real need to push the limits of what we can measure, and clever schemes are needed to quantitatively measure released substances that are not easily oxidized (or reduced). These sensors will need to be extremely sensitive and to give a response that is one to one with the number of molecules similarly to amperometry. This is a huge challenge and one that might be taken on by the enzyme electrode area.

Acknowledgments The authors thank the Swedish Research Council (VR) for support. AGE gratefully acknowledges support from the European Research Council (ERC), the Knut and Alice Wallenberg Foundation, and the USA National Institutes of Health.

References

1. Alvarez de Toledo G, Fernandez-Chacon R, Fernandez JM (1993) Nature 363:554–558
2. Amatore C, Arbault S, Bonifas I, Lemaitre F, Verchier Y (2007) Chemphyschem 8:578–585
3. Amatore C, Arbault S, Bouret Y, Guille M, Lemaitre F, Verchier Y (2006) Chembiochem 7:1998–2003
4. Anderson BB, Chen G, Gutman DA, Ewing AG (1999) J Neurosci Methods 88:153–161
5. Chen G, Gavin PF, Luo G, Ewing AG (1995) J Neurosci 15:7747–7755
6. Chow RH, von Ruden L, Neher E (1992) Nature 356:60–63
7. Colliver TL, Pyott SJ, Achalabun M, Ewing AG (2000) J Neurosci 20:5276–5282
8. Leszczyszyn DJ, Jankowski JA, Viveros OH, Diliberto EJ Jr, Near JA, Wightman RM (1990) J Biol Chem 265:14736–14737
9. Sombers LA, Maxson MM, Ewing AG (2005) J Neurochem 93:1122–1131
10. Uchiyama Y, Maxson MM, Sawada T, Nakano A, Ewing AG (2007) Brain Res 1151:46–54
11. Westerink RH, de Groot A, Vijverberg HP (2000) Biochem Biophys Res Commun 270:625–630
12. Wightman RM, Jankowski JA, Kennedy RT, Kawagoe KT, Schroeder TJ, Leszczyszyn DJ, Near JA, Diliberto EJ, Viveros OH (1991) Proc Natl Acad Sci USA 88:10754–10758
13. Wightman RM, Schroeder TJ, Finnegan JM, Ciolkowski EL, Pihel K (1995) Biophys J 68:383–390
14. Finnegan JM, Pihel K, Cahill PS, Huang L, Zerby SE, Ewing AG, Kennedy RT, Wightman RM (1996) J Neurochem 66:1914–1923
15. Albillos A, Dernick G, Horstmann H, Almers W, Alvarez de Toledo G, Lindau M (1997) Nature 389:509–512
16. Chen TK, Luo G, Ewing AG (1994) Anal Chem 66:3031–3035
17. Hochstetler SE, Puopolo M, Gustincich S, Raviola E, Wightman RM (2000) Anal Chem 72:489–496
18. Pothos EN (2002) Behav Brain Res 130:203–207
19. Staal RG, Mosharov EV, Sulzer D (2004) Nat Neurosci 7:341–346
20. Zhang Q, Li Y, Tsien RW (2009) Science 323:1448–1453
21. Ciolkowski EL, Cooper BR, Jankowski JA, Jorgenson JW, Wightman RM (1992) J Am Chem Soc 114:2815–2821
22. Dayton MA, Brown JC, Stutts KJ, Wightman RM (1980) Anal Chem 52:946–950
23. Wightman RM (2006) Science 311:1570–1574
24. Heien ML, Johnson MA, Wightman RM (2004) Anal Chem 76:5697–5704
25. Camacho M, Machado JD, Montesinos MS, Criado M, Borges R (2006) J Neurochem 96:324–334
26. Haynes CL, Buhler LA, Wightman RM (2006) Biophys Chem 123:20–24
27. Pothos EN, Mosharov E, Liu K-P, Setlik W, Haburcak M, Baldini G, Gershon MD, Tamir H, Sulzer D (2002) J Physiol 542:453–476
28. Holz RW, Senter RA, Frye RA (1982) J Neurochem 39:635–646
29. Livett BG (1984) Physiol Rev 64:1103–1161
30. Heuser JE, Reese TS, Dennis MJ, Jan Y, Jan L, Evans L (1979) J Cell Biol 81:275–300
31. Fesce R, Grohovaz F, Hurlbut WP, Ceccarelli B (1980) J Cell Biol 85:337–345
32. Heuser JE, Reese TS (1981) J Cell Biol 88:564–580
33. Chandler DE, Heuser JE (1980) J Cell Biol 86:666–674
34. Schneider SW, Sritharan KC, Geibel JP, Oberleithner H, Jena BP (1997) Proc Natl Acad Sci USA 94:316–321
35. Neher E, Marty A (1982) Proc Natl Acad Sci USA 79:6712–6716

36. Haller M, Heinemann C, Chow RH, Heidelberger R, Neher E (1998) Biophys J 74:2100–2113
37. Dernick G, Alvarez de Toledo G, Lindau M (2003) Nat Cell Biol 5:358–362
38. Sombers LA, Hanchar HJ, Colliver TL, Wittenberg N, Cans A, Arbault S, Amatore C, Ewing AG (2004) J Neurosci 24:303–309
39. Evans E, Bowman H, Leung A, Needham D, Tirrell D (1996) Science 273:933–935
40. Hoekstra D (1990) Hepatology 12:61S–66S
41. Kahya N, de Pecheur EI, Boeij WP, Wiersma DA, Hoekstra D (2001) Biophys J 81:1464–1474
42. Woodbury DJ (1999) Cell Biochem Biophys 30:303–329
43. Zimmerberg J, Cohen FS, Finkelstein A (1980) J Gen Physiol 75:241–250
44. Chanturiya A, Chernomordik LV, Zimmerberg J (1997) Proc Natl Acad Sci USA 94:14423–14428
45. Cans AS, Wittenberg N, Karlsson R, Sombers L, Karlsson M, Orwar O, Ewing AG (2003) Proc Natl Acad Sci USA 100:400–404
46. Cans AS, Wittenberg N, Eves D, Karlsson R, Karlsson A, Orwar O, Ewing AG (2003) Anal Chem 75:4168–4175
47. Karlsson M, Nolkrantz K, Davidson MJ, Stromberg A, Ryttsen F, Akerman B, Orwar O (2000) Anal Chem 72:5857–5862
48. Fisher RJ, Pevsner J, Burgoyne RD (2001) Science 291:875–878
49. Voets T, Toonen RF, Brian EC, de Wit H, Moser T, Rettig J, Sudhof TC, Neher E, Verhage M (2001) Neuron 31:581–591
50. Borisovska M, Zhao Y, Tsytsyura Y, Glyvuk N, Takamori S, Matti U, Rettig J, Sudhof T, Bruns D (2005) EMBO J 24:2114–2126
51. Westerink RH (2004) Neurotoxicology 25:461–470
52. Borges R, Machado JD, Betancor G, Camacho M (2002) Ann NY Acad Sci 971:184–192
53. Kozminski KD, Gutman DA, Davila V, Sulzer D, Ewing AG (1998) Anal Chem 70:3123–3130
54. Westerink RHS, Ewing AG (2008) Acta Physiol 192:273–285
55. Amatore C, Arbault S, Bonifas I, Guille M, Lemaitre F, Verchier Y (2007) Biophys Chem 129:181–189
56. Dernick G, Gong LW, Tabares L, Alvarez de Toledo G, Lindau M (2005) Nat Meth 2:699–708
57. Edwards RH (2007) Neuron 55:835–858
58. Schroeder TJ, Jankowski JA, Senyshyn J, Holz RW, Wightman RM (1994) J Biol Chem 269:17215–17220
59. Zhang B, Adams KL, Luber SJ, Eves DJ, Heien ML, Ewing AG (2008) Anal Chem 80:1394–1400
60. Amatore C, Arbault S, Lemaitre F, Verchier Y (2007) Biophys Chem 127:165–171
61. Woods LA, Gandhi PU, Ewing AG (2005) Anal Chem 77:1819–1823
62. Omiatek DM, Santillo MF, Heien ML, Ewing AG (2009) Anal Chem 81:2294–2302
63. Omiatek DM, Dong Y, Heien ML, Ewing AG (2010) ACS Chem Neurosci 1:234–245
64. Hirschberg K, Miller CM, Ellenberg J, Presley JF, Siggia ED, Phair RD, Lippincott-Schwartz J (1998) J Cell Biol 143:1485–1503
65. Polishchuk RS, Polishchuk EV, Marra P, Alberti S, Buccione R, Luini A, Mironov AA (2000) J Cell Biol 148:45–58
66. Onfelt B, Nedvetzki S, Yanagi K, Davis DM (2004) J Immunol 173:1511–1513
67. Rustom A, Saffrich R, Markovic I, Walther P, Gerdes HH (2004) Science 303:1007–1010
68. Adams KL, Engelbrektsson J, Voinova M, Zhang B, Eves DJ, Karlsson R, Heien ML, Cans AS, Ewing AG (2010) Anal Chem 82:1020–1026
69. Haynes CL, Siff LN, Wightman RM (2007) Mol Cell Res 1773:728–735
70. Wightman RM, Haynes CL (2004) Nat Neurosci 7:321–322